Since January 2020 Elsevier has created a COVID-19 resource centre with free information in English and Mandarin on the novel coronavirus COVID-19. The COVID-19 resource centre is hosted on Elsevier Connect, the company's public news and information website.

Biosensors and Bioelectronics 172 (2021) 112705

Contents lists available at ScienceDirect

Biosensors and Bioelectronics

journal homepage: http://www.elsevier.com/locate/bios

Introducing polymer conductance in diagnostically relevant transduction

Ausra Baradoke [a], Adriano Santos [b], Paulo R. Bueno [b,*], Jason J. Davis [a,**]

[a] Department of Chemistry, University of Oxford, South Parks Road, Oxford OX1 3QZ, United Kingdom
[b] Institute of Chemistry, São Paulo State University (UNESP), 14800-060, Araraquara, São Paulo, Brazil

ARTICLE INFO

Keywords:
Point-of-care
Molecular scale conductance
Biosensors
Reagentless
C-reactive protein

ABSTRACT

In this work we demonstrate that an impedance derived capacitance method is able to cleanly resolve the resonant conductance characteristics of an electrode-confined polymer film. In decorating the film with receptors, this conductance is thereafter modulated by the capturing of specific targets, demonstrated herein with C-reactive protein. This entirely reagentless and single step marker quantification is relevant to the drive of moving assays to a scaleable format requiring minimal user intervention.

1. Introduction

The considerable growth, aging and increased mobility of the human population is driving a progressive demand for more responsive, lower cost, health services, additionally able to support earlier intervention (Cėpla et al., 2020; Guo 2012; Piliarik et al., 2009). Infection outbreaks, such as those caused by influenza virus (H1N1) (Dotis and Roilides, 2009) and SARS-CoV-2 (Bedford et al., 2020), are very specific recent examples of the need to screen and monitor public health; any such capability must necessarily be underpinned by a reliable and scaleable assaying platform that requires minimal user intervention. Within this space, technologies which are "label-free" are particularly attractive and a range of such methods are available based on optically resolved dielectric change (surface plasmon resonance (Cėpla et al., 2020; Guo 2012), piezoelectric based mass detection (quartz crystal microbalance) (Speight and Cooper 2012) and electrochemistry (Baradoke et al., 2019b; da Silva et al., 2017; Grieshaber et al., 2008; Kimmel et al., 2011; Ronkainen et al., 2010). Of the electrochemical methods, those based on impedance spectroscopy (EIS), can be exceedingly sensitive and derived capacitive methods (ECS) equally so without any requirement for a redox probe in solution (Fernandes et al., 2014; Garrote et al., 2019). Where traditional EIS sensors primarily monitor changes in the charge transfer resistance (R_{ct}) upon a target binding event (Baradoke et al., 2019a; Lisdat and Schäfer 2008; Santos et al., 2014) these require the addition of a large excess of diffusively mobile redox probe to solution and are limited in terms of scope of supporting film (making the use of multifunctional or highly nonfouling interfaces, more than a few nanometres in thickness, difficult). ECS, on the other hand, monitors changes in the charging state of the interface. We have shown that this can be evaluated by using the electrochemical capacitance ($C_{\bar{\mu}}$) signal of the interface (Bueno et al. 2012, 2013; Fernandes et al., 2013). $C_{\bar{\mu}}$ is mesoscopic in essence (Bueno 2018a, b, 2019; Bueno and Davis 2020) and related to the redox density-of-states (DOS) of film-confined redox addressable functionalities. This faradaically derived capacitive signal can be used in derived clinically relevant biomarker assays with ferrocene based monolayers, mixed films, peptides and Prussian blue decorated interfaces (Cecchetto et al., 2020; Fernandes et al., 2014; Santos et al., 2014). Herein we demonstrate the resonant conductance of the film associated with the redox capacitive states can also be used to transduce local binding events in an entirely "reagentless" manner.

In order to charge/discharge electrode-confined redox states, such as those presented by a faradaically-active polymer film, they must be electronically addressable from the electrode such that the imposition of a specific dV promotes a resonant exchange of electrons. If a sinusoidal wave is superimposed on this bias the interfacial capacitance is readily mapped, as is the conductance across the "molecular bridge" spanning the space between electrode and redox site (Bueno and Davis 2020). The chemical potential of this bridge is related to the potential gradient through $dV = -d\mu/e$, where e is the elementary charge. For an ideal quantum mechanical single electrical channel, the current is $di = -d\mu(ev/L)(\delta N/\delta\mu)$, where N is the number of electrons, and v the charge velocity component along the channel length L. Importantly, in this mesoscopic regime of scale, the "bridge" electronic properties show a dependency on the bridge DOS through $(\delta N/\delta\mu) = 2L/hv$ (h is

* Corresponding author.
** Corresponding author.
E-mail addresses: paulo-roberto.bueno@unesp.br (P.R. Bueno), jason.davis@chem.ox.ac.uk (J.J. Davis).

https://doi.org/10.1016/j.bios.2020.112705
Received 27 August 2020; Received in revised form 30 September 2020; Accepted 6 October 2020
Available online 22 October 2020
0956-5663/

the Planck constant). This DOS is, in turn, spatially and energetically coupled to that of the (faradaically charging) redox sites in a manner that governs the charge and discharge characteristics of the film, where the associated electric current can be expressed as $di = N(2e^2/h)dV$. Consequently, one can write $i = NG_0V$, where $NG_0 = 2Ne^2/h$ and $G_0 = 2e^2/h$ is the quantum of conductance. For a (realistic) transmittance through multiple channels, the arising mesoscopic conductance G is given by $G = G_0\sum_n T_n(\mu) = NG_0$, where $\sum_n T_n(\mu)$ represents the overall transmission probability across the "molecular bridge" and equates to N if the transmittance of the individual channels is ideal. A key part of this formalism is that any change in $C_{\bar{\mu}}$ (such as that induced by a local target capture event) will alter the mesoscopic conductance G of the bridge.

Traditional EIS, encompassing an analysis of the charge transfer between electrode and free species in solution (in parallel to double layer capacitance), does not report on resonant conductance/resistance because the latter requires that the DOS exchanging electrons with the electrode is electronically and mechanically coupled to it, not in solution. Even in the absence of a traditional solution phase redox probe, a standard impedimetric Nyquist analysis of an electrode coupled conductive film fails to resolve any meaningful film resistance (Fig. 1c; where only solution resistance, R_s, is resolvable). For this we revert to a capacitance analysis. We note first that $C_{\bar{\mu}}$ is given by the diameter of a capacitive Nyquist semicircle (Fig. 1d) and that $C_{\bar{\mu}}$ dominates over C_{dl}, for redox addressable films (where the double layer charging is heavily suppressed). The resistive component of the charging element R_q is accessed through a Bode analysis noting that $\tau^{-1} = 1/(R_s + R_{ct})C_{\bar{\mu}}$, where the inverse corresponds to an RC time constant and peak frequency $f_p = 1/(2\pi\tau)$ (Fig. 1e). Film conductance is, of course, $G = 1/R_q$. This R_q, recorded when film redox states are resonant with electrode states, corresponds to the higher limit of the conductance (Fig. 2b), but can thereafter be modulated by any change in bridge chemical potential; these changes are induced by localised (recognition) effects at the electronically coupled redox sites.

In prior work we have demonstrated that the capacitive analysis of redox addressable and target receptive films can be applied in signal transduction (Fernandes et al., 2013; Oliveira et al., 2019; Piccoli et al., 2018; Santos et al., 2015), and that there is an intrinsic association between resolved molecular film capacitance and film conductance (Bueno 2018a, b; Bueno and Davis 2020). Herein we demonstrate that, with suitably prepared conductive polymer films, the recruitment of targets is associated with a measurable change in film chemical potential and thus conductance. Such "conductometric" analyses have classically been restricted to field-effect transistor (FET) configurations. Although these possess an inherent amplification, they also require very substantial control over microfabrication and can be problematic to reproducibly scale when interfaces with aqueous biology. The conductance analyses herein are "single electrode contact" in basis and very readily scaled. We exemplify this here with a redox charging conductive polyaniline film and a quantification of C-reactive protein biomarker (CRP), a cardiac, acute phase, and inflammatory marker (Black et al., 2004).

2. Experimental

Details of the screen-printed electrodes and reagents are described in Supplementary Information (SI-1 & SI-6).

All electrochemical experiments were performed with a portable PalmSens potentiostat in a three-electrode configuration, consisting of a screen-printed graphene ink working electrode (SPE), a screen-printed silver reference electrode, and a screen-printed gold counter electrode. All experiments were performed in 0.1 M phosphate buffer (PB), pH 7.4, unless otherwise stated.

EIS was performed between 9 kHz and 0.1 Hz (20 frequencies logarithmic arranged), with a sigmoidal AC perturbation of 10 mV (peak-to-peak). These experiments were performed at the "redox in" or formal DC potential of the PANI film (−0.2 V). Capacitance data was obtained via $C'(\omega) = Z''/\omega|Z|^2$ and $C''(\omega) = Z'/\omega|Z|^2$, where ω is the angular frequency ($\omega = 2\pi f$). The $C_{\bar{\mu}}$ of the interface was obtained graphically as the diameter of the semicircle of the capacitive Nyquist plots. The conductance G was calculated from the resistance R_q as determined from the peak frequency f_p of the imaginary capacitance Bode plot ($\tau^{-1} = 1/[(R_s + R_q)C_{\bar{\mu}}] = 2\pi f_p$) as shown in Fig. 1e as example). Note that $G = 1/R_q$, and that, additionally, R_s can be obtained from the impedimetric Nyquist plot at high frequencies (as shown in Fig. 1c) (Lisdat and Schäfer, 2008). The relative response $RR(\%)$ for the signal transduction G was obtained as follows $RR(\%) = (G_{[target]} - G_{blank})/G_{blank}$, where $G_{[target]}$ is the signal transduction for a certain target concentration, and G_{blank} is the signal of the blank. The limit of detection (LOD) of the assay was defined by $LOD = 3\,\sigma/slope$, where σ is the standard deviation of the y-intercept of the standard plot ($RR(\%)$ versus target concentration) (Shrivastava and Gupta, 2011).

2.1. Sensor interface generation

Electrodes were washed with copious amounts of water, followed by electrochemical polishing in 0.1 M KOH, between −1.0 V to 1.3 V for 20 cycles. Electropolymerisation of pythic acid doped polyaniline (PANI-Pa) was performed in an aqueous solution of 1 mL 98% aniline and 2 mL of 50% phytic acid (w/w in H_2O) with the addition of 17 mL of MilliQ water by applying a current density of 10 μA/cm^2 for 10 min. The film

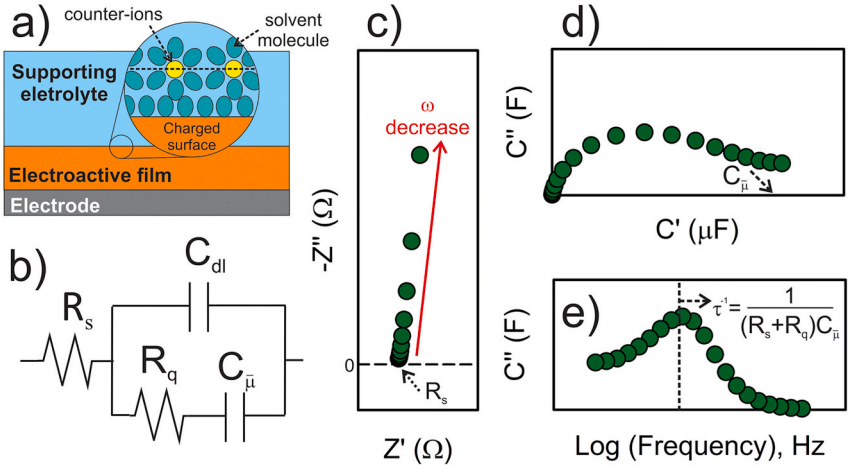

Fig. 1. For a charged electrode-modified electroactive film immersed in a supporting electrolyte (a) the electrochemical features of the interface can be modelled by an equivalent circuit comprising solution resistance R_s connected in series with a parallel combination of the C_{dl} and R_q in series with $C_{\bar{\mu}}$ (b). A typical impedance response is shown in (c), which can be usefully transformed into the capacitance domain (d). R_s can be obtained at high frequencies ($\omega = 2\pi f$), as shown in (c) $C_{\bar{\mu}}$ can be then estimated by the diameter of the semicircle. (e) Bode plot for the imaginary part of the capacitance as the function of frequency. The peak frequency f_q can be used to estimate R_q.

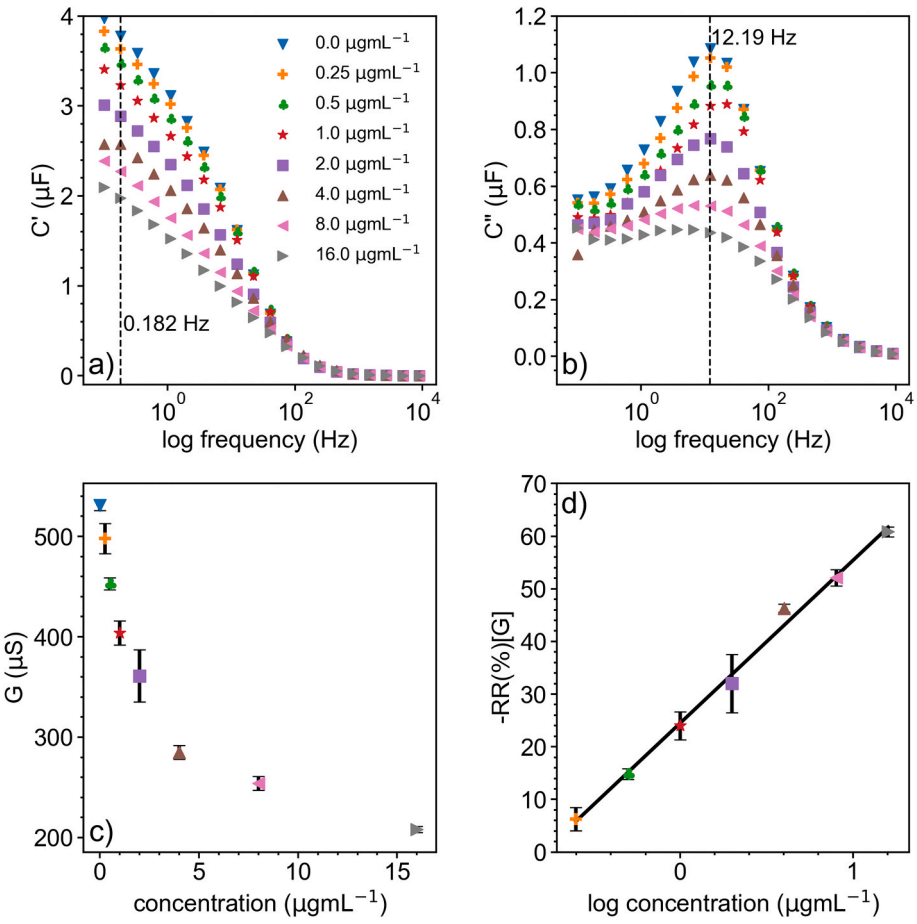

Fig. 2. (a) Real $C^{'}$ and (b) Imaginary C'' components of complex capacitance vs. frequency (Bode plots) after sensor exposure to CRP in 1% fetal bovine serum. Frequency peak (f_p) used for G calculation is shown in (b). (c) The film conductance G (μS) responses on exposure to different target concentrations. (d) A representative calibration curve derived from (c) with $R^2 = 0.994$. Error bars represent standard deviation from independent measurements.

was rinsed with 0.1 M PB and then equilibrated in the same buffer for 10 min before further electrochemical characterization. Covalent immobilization of the receptor was performed by exposure of the PANI-PA films to 2.5% glutaraldehyde (in PB) for 30 min, followed by rinsing with copious amounts of PB and exposure to 5 μg mL^{-1} of anti-CRP or 5 μg mL^{-1} anti-D-dimer for 30 min. After rinsing with 0.1 M PB (pH 7.4), remaining active sites were deactivated with 10 mM ethanolamine in 0.1 M PB (pH 7.4) for 30 min, followed by rinsing with PB.

2.2. Immunoassay

Sensor surfaces were first equilibrated in PB for 30 min. Prior to a 10-min exposure to defined target concentrations (from 0.25 μg mL^{-1} to 16 μg mL^{-1}) or control proteins, both spiked into 1% fetal bovine serum (FBS). Sensors were then rinsed in PB and $C_{\bar{\mu}}$, τ, and R_s recorded in pure PB in order to obtain conductance of the film for each target concentration.

3. Results and discussion

In generating antibody supporting conductive films, aqueous phase electrodeposition generates a stable electroactive film presenting an oxidation potential peak (V_{ox}) at about -0.15 V, and reduction potential peak (V_{red}) at about -0.25 V in PB solution (Figure SI-1a, in Supplementary Information). $C_{\bar{\mu}}$ is resolved to be, as expected, maximal at the electrochemical formal potential (~32 μF from the semicircle diameter in Figure SI-1b). In the absence of PANI-Pa a resolved (geometric) double layer capacitance is ~0.3 μF.

A subsequent standard glutaraldehyde coupling of anti-CRP results in a decrease in $C_{\bar{\mu}}$ (Figure SI-2), related to the attenuation of the redox signal as expected (Fernandes et al. 2013, 2014; Lehr et al., 2014). As shown in Fig. 2a and Figure SI-3, $C_{\bar{\mu}}$ thereafter decreases as target concentrations increases (visualized at ~0.182 Hz, the frequency where the real component of the complex capacitance produces the semicircle from which $C_{\bar{\mu}}$ is obtained). By analyzing the circuit elements from the Nyquist and Bode capacitive plots and frequency peak (f_p), film conductance can be resolved to decrease on specific target recruitment (Table SI-1). This conductance decrease/resistance increase is consistent with the observed decrease in coupled electrochemical capacitance (Figure SI-3) which in turn directly reflects the current through the "bridge", noting that $di = -d\mu(ev/L)(\delta N/\delta\mu)$, where $\delta N/\delta\mu$ is DOS.

A plot of interfacial relative response $(RR(\%) = (G_{[target]} - G_{blank})/G_{blank})$ generates a standard curve (Fig. 2d), with a resolved sensitivity at least as good as that typically reported for capacitance sensors (Baradoke et al., 2020; Piccoli et al., 2018) and a limit of detection (LOD) of 1.8 μg mL^{-1} (10 nmol L^{-1}) that is clinically relevant (Sonawane and Nimse, 2017). Interfacial conductance responses show good levels of selectivity (Figure SI-4b) and can be accurately ($R^2 > 0.99$) described by the Langmuir-type isotherm (Figure SI-4a), with a dissociation constant entirely consistent with previous reports with a $k_d = 17\ nM$ (Baradoke et al., 2020).

4. Conclusion

We have herein demonstrated that the conductance of an electrode-confined redox polymer can be used as a transducer signal for

biosensing. This conductance is directly correlated to the electrochemical or redox capacitance of the film that arises from its embedded faradaically-active sites. Following a relationship theoretically outlined in previous work (Bueno 2018a, b; Bueno and Davis 2020) these principles represent a highly accessible, readily scaleable, single electrode contact, field effect sensing ability.

CRediT authorship contribution statement

Ausra Baradoke: Methodology, Data curation. **Adriano Santos:** Methodology, Data curation, Conceptualization, Writing - review & editing, Writing. **Paulo R. Bueno:** Conceptualization, Supervision, Resources, Methodology, Writing - original draft. **Jason J. Davis:** Conceptualization, Supervision, Resources, Methodology, Writing - original draft.

Declaration of competing interest

The authors declare that they have no known competing financial interests or personal relationships that have influenced the work reported in this paper.

Acknowledgments

J.J.D would like to thank Innovate UK and Osler Diagnostics for funding. P.R.B. and A.S. would like to thank FAPESP and CAPES.

Appendix A. Supplementary data

Supplementary data to this article can be found online at https://doi.org/10.1016/j.bios.2020.112705.

References

Baradoke, A., Hein, R., Li, X., Davis, J.J., 2020. Reagentless redox capacitive assaying of CRP at a polyaniline interface. Anal. Chem.
Baradoke, A., Jose, B., Pauliukaite, R., Forster, R.J., 2019a. Properties of Anti-CA125 antibody layers on screen-printed carbon electrodes modified by gold and platinum nanostructures. Electrochim. Acta 306, 299–306.
Baradoke, A., Pastoriza-Santos, I., González-Romero, E., 2019b. Screen-printed GPH electrode modified with Ru nanoplates and PoPD polymer film for NADH sensing: design and characterization. Electrochim. Acta 300, 316–323.
Bedford, J., Enria, D., Giesecke, J., Heymann, D.L., Ihekweazu, C., Kobinger, G., Lane, H. C., Memish, Z., Oh, M.-d., Sall, A.A., Schuchat, A., Ungchusak, K., Wieler, L.H., 2020. COVID-19: towards controlling of a pandemic. Lancet 395 (10229), 1015–1018.
Black, S., Kushner, I., Samols, D., 2004. C-reactive protein. J. Biol. Chem. 279 (47), 48487–48490.
Bueno, P.R., 2018a. Common principles of molecular electronics and nanoscale electrochemistry. Anal. Chem. 90 (12), 7095–7106.
Bueno, P.R., 2018b. The Nanoscale Electrochemistry of Molecular Contacts. Springer.
Bueno, P.R., 2019. Nanoscale origins of super-capacitance phenomena. J. Power Sources 414, 420–434.
Bueno, P.R., Davis, J.J., 2020. Charge transport and energy storage at the molecular scale; from nanoelectronics to electrochemical sensing. Chem. Rev.
Bueno, P.R., Fabregat-Santiago, F., Davis, J.J., 2013. Elucidating capacitance and resistance terms in confined electroactive molecular layers. Anal. Chem. 85 (1), 411–417.
Bueno, P.R., Mizzon, G., Davis, J.J., 2012. Capacitance spectroscopy: a versatile approach to resolving the redox density of states and kinetics in redox-active self-assembled monolayers. J. Phys. Chem. B 116 (30), 8822–8829.
Cecchetto, J., Santos, A., Mondini, A., Cilli, E.M., Bueno, P.R., 2020. Serological point-of-care and label-free capacitive diagnosis of dengue virus infection. Biosens. Bioelectron. 151, 111972.
Cėpla, V., Rakickas, T., Stankevičienė, G., Mazėtytė-Godienė, A., Baradokė, A., Ruželė, Ž., Valiokas, R.n., 2020. Photografting and patterning of poly(ethylene glycol) methacrylate hydrogel on glass for biochip applications. ACS Appl. Mater. Interfaces 12 (29), 32233–32246.
da Silva, E., Souto, D.E.P., Barragan, J.T.C., Giarola, J.D., de Moraes, A.C.M., Kubota, L. T., 2017. Electrochemical biosensors in point-of-care devices: recent advances and future trends. ChemElectroChem 4 (4), 778–794.
Dotis, J., Roilides, E., 2009. H1N1 influenza A infection. Hippokratia 13 (3), 135–138.
Fernandes, F.C.B., Góes, M.S., Davis, J.J., Bueno, P.R., 2013. Label free redox capacitive biosensing. Biosens. Bioelectron. 50, 437–440, 0.
Fernandes, F.C.B., Santos, A., Martins, D.C., Góes, M.S., Bueno, P.R., 2014. Comparing label free electrochemical impedimetric and capacitive biosensing architectures. Biosens. Bioelectron. 57, 96–102, 0.
Garrote, B.L., Santos, A., Bueno, P.R., 2019. Perspectives on and precautions for the uses of electric spectroscopic methods in label-free biosensing applications. ACS Sens. 4 (9), 2216–2227.
Grieshaber, D., MacKenzie, R., Voros, J., Reimhult, E., 2008. Electrochemical biosensors - sensor principles and architectures. Sensors 8 (3), 1400–1458.
Guo, X., 2012. Surface plasmon resonance based biosensor technique: a review. J. Biophot. 5 (7), 483–501.
Kimmel, D.W., LeBlanc, G., Meschievitz, M.E., Cliffel, D.E., 2011. Electrochemical sensors and biosensors. Anal. Chem. 84 (2), 685–707.
Lehr, J., Fernandes, F.C.B., Bueno, P.R., Davis, J.J., 2014. Label-free capacitive diagnostics: exploiting local redox probe state occupancy. Anal. Chem. 86 (5), 2559–2564.
Lisdat, F., Schäfer, D., 2008. The use of electrochemical impedance spectroscopy for biosensing. Anal. Bioanal. Chem. 391 (5), 1555.
Oliveira, R.M.B., Fernandes, F.C.B., Bueno, P.R., 2019. Pseudocapacitance phenomena and applications in biosensing devices. Electrochim. Acta 306, 175–184.
Piccoli, J., Hein, R., El-Sagheer, A.H., Brown, T., Cilli, E.M., Bueno, P.R., Davis, J.J., 2018. Redox capacitive assaying of C-reactive protein at a peptide supported aptamer interface. Anal. Chem. 90 (5), 3005–3008.
Piliarik, M., Vaisocherová, H., Homola, J., 2009. Surface plasmon resonance biosensing. In: Rasooly, A., Herold, K.E. (Eds.), Biosensors and Biodetection. Humana Press, Totowa, NJ, pp. 65–88.
Ronkainen, N.J., Halsall, H.B., Heineman, W.R., 2010. Electrochemical biosensors. Chem. Soc. Rev. 39 (5), 1747–1763.
Santos, A., Davis, J.J., Bueno, P.R., 2014. Fundamentals and applications of impedimetric and redox capacitive biosensors, 0(0). J. Anal. Bioanal. Tech.
Santos, A., Piccoli, J.P., Santos-Filho, N.A., Cilli, E.M., Bueno, P.R., 2015. Redox-tagged peptide for capacitive diagnostic assays. Biosens. Bioelectron. 68, 281–287.
Shrivastava, A., Gupta, V., 2011. Methods for the determination of limit of detection and limit of quantitation of the analytical methods. Chronicles Young Sci. 2 (1), 21–25.
Sonawane, M.D., Nimse, S.B., 2017. C-Reactive protein: a major inflammatory biomarker. Anal. Methods 9 (23), 3400–3413.
Speight, R.E., Cooper, M.A., 2012. A survey of the 2010 quartz crystal microbalance literature. J. Mol. Recogn. 25 (9), 451–473.